Deficiency in the LIM-only protein Fhl2 impairs skin wound healing

Viktor Wixler,[1] Stephanie Hirner,[3] Judith M. Müller,[4] Lucia Gullotti,[3] Carola Will,[1] Jutta Kirfel,[3] Thomas Günther,[4] Holm Schneider,[5] Anja Bosserhoff,[6] Hubert Schorle,[2] Jung Park,[7] Roland Schüle,[4] and Reinhard Buettner[3]

[1]Institute of Molecular Virology, Münster University Hospital Medical School, D-48149 Münster, Germany
[2]Department of Developmental Pathology, [3]Institute of Pathology, University Hospital Medical School, D-53127 Bonn, Germany
[4]Center for Clinical Research, University of Freiburg, D-79106 Freiburg, Germany
[5]Experimental Neonatology, Department of Pediatrics, Medical University of Innsbruck, Innrain 66, A-6020 Innsbruck, Austria
[6]Institute of Pathology, University Hospital Regensburg, D-93042 Regensburg, Germany
[7]Department of Experimental Medicine I, University of Erlangen-Nürnberg, D-91054 Erlangen, Germany

After skin wounding, the repair process is initiated by the release of growth factors, cytokines, and bioactive lipids from injured vessels and coagulated platelets. These signal molecules induce synthesis and deposition of a provisional extracellular matrix, as well as fibroblast invasion into and contraction of the wounded area. We previously showed that sphingosine-1-phosphate (S1P) triggers a signal transduction cascade mediating nuclear translocation of the LIM-only protein Fhl2 in response to activation of the RhoA GTPase (Muller, J.M., U. Isele, E. Metzger, A. Rempel, M. Moser, A. Pscherer, T. Breyer, C. Holubarsch, R. Buettner, and R. Schule. 2000. *EMBO J.* 19:359–369; Muller, J.M., E. Metzger, H. Greschik, A.K. Bosserhoff, L. Mercep, R. Buettner, and R. Schule. 2002. *EMBO J.* 21:736–748.). We demonstrate impaired cutaneous wound healing in *Fhl2*-deficient mice rescued by transgenic expression of Fhl2. Furthermore, collagen contraction and cell migration are severely impaired in *Fhl2*-deficient cells. Consequently, we show that the expression of α-smooth muscle actin, which is regulated by Fhl2, is reduced and delayed in wounds of *Fhl2*-deficient mice and that the expression of p130Cas, which is essential for cell migration, is reduced in *Fhl2*-deficient cells. In summary, our data demonstrate a function of Fhl2 as a lipid-triggered signaling molecule in mesenchymal cells regulating their migration and contraction during cutaneous wound healing.

Introduction

In recent years, considerable progress has been made in understanding the role of growth factors and cytokines in wound healing. These factors are released from injured vessels and coagulated platelets and trigger an inflammatory response that initiates the deposition of a provisional extracellular matrix. In parallel, mesenchymal and endothelial precursor cells invade the wound to form the granulation tissue and to contract the wounded area.

Contraction of the granulation tissue by mesodermal fibroblasts is of high importance for sealing the wound, as it helps to bring the wound margins together. To be able to contract efficiently, mesenchymal cells of the granulation tissue differentiate into myofibroblasts characterized by a well-developed cytoskeleton. Myofibroblasts express α-smooth muscle actin (α-SMA), which is incorporated into actin stress fibers and enables them to develop much higher mechanical forces (Hinz and Gabbiani, 2003). Hence, induction of α-SMA expression in fibroblasts is a critical step in wound healing.

Besides growth factors and cytokines, bioactive lipids have been identified as important signal molecules, modulating inflammatory responses, cell growth, and tissue formation. However, the role of lipid-induced signaling and its contribution to wound healing is still poorly understood. We previously showed that sphingosine-1-phosphate (S1P) triggers a signal transduction cascade mediating nuclear translocation of the LIM-only protein Fhl2 in response to activation of the RhoA GTPase (Muller et al., 2000, 2002). We and others further identified the LIM-only protein Fhl2 as interacting with transcription factors, including androgen receptor (Muller et al., 2002), serum response factor (SRF; Philippar et al., 2004; Purcell et al., 2004), Jun, and Fos (Morlon and Sassone-Corsi, 2003), as well as with integrin receptors (Wixler et al., 2000; Samson et al., 2004)

V. Wixler, S. Hirner, J.M. Müller, and L. Gullotti contributed equally to this paper.

Correspondence to Reinhard Buettner: Reinhard.Buettner@ukb.uni-bonn.de

Abbreviations used in this paper: HEK, human embryonic kidney; S1P, sphingosine-1-phosphate; SMA, smooth muscle actin; SRF, serum response factor.

The online version of this article contains supplemental material.

The Journal of Cell Biology, Vol. 177, No. 1, April 9, 2007 163–172
http://www.jcb.org/cgi/doi/10.1083/jcb.200606043

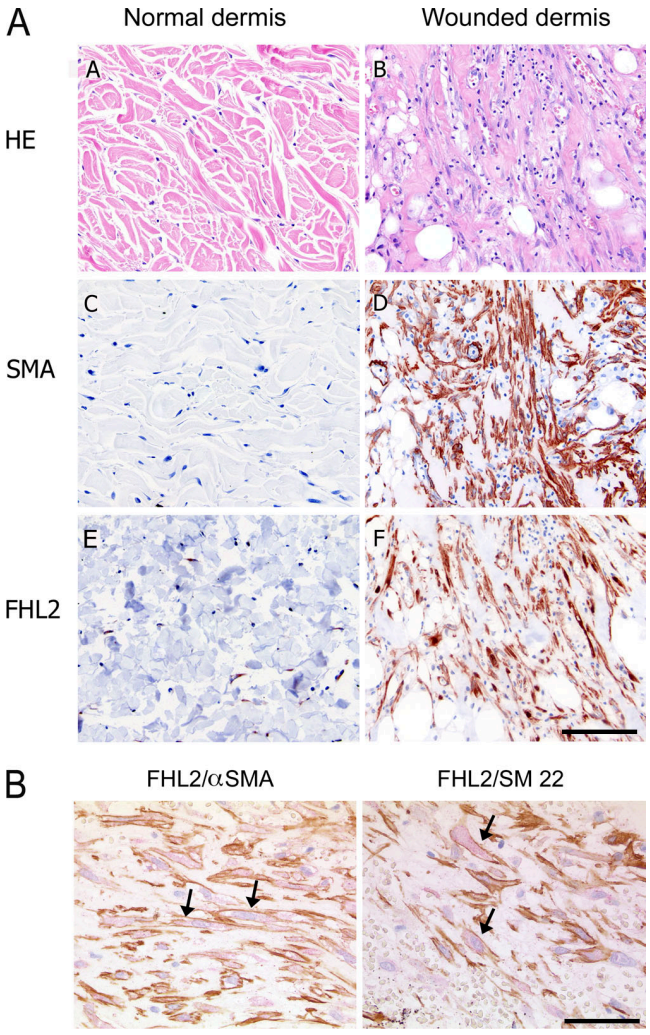

Figure 1. **Expression and nuclear translocation of Fhl2 in myofibroblasts within human skin wounds.** (A) Immunostaining of human wound tissue reveals strong up-regulation of Fhl2 in α-SMA–positive myofibroblast-like cells present in dermal granulation tissue 5 d after wounding. (B) Double immunostaining of human wound tissue indicates that Fhl2 immunosignals (arrows, red AEC stain) label α-SMA– and SM22-positive myofibroblasts. Bars: (A) 50 μm; (B) 25 μm.

and signal transducers such as β-catenin (Martin et al., 2002). Fhl2 associates with integrins at focal adhesion sites and is translocated into the nucleus upon stimulation by serum or S1P to modulate transcriptional activity of numerous target genes. Because significant amounts of S1P and lysophosphatidic acid are released from platelets during tissue repair (Yatomi et al., 2000), we investigated the role of Fhl2 signaling in mesenchymal cells during wound healing.

Results

Previous studies of Fhl2 in prostate cancer revealed its expression in the prostate cancer cells proper, but also in myofibroblast-like cells within the stroma (Muller et al., 2000, 2002). To confirm expression and regulation of Fhl2 in mesenchymal cells, we isolated primary embryonic mouse fibroblasts and visualized Fhl2 expression and nuclear translocation in response to serum exposure. When fibroblasts were starved in 0.5% FCS, and then exposed to 10% FCS for 24 and 48 h, respectively, we observed both significant up-regulation of Fhl2 mRNA and nuclear translocation of the respective protein (Fig. S1, available at http://www.jcb.org/cgi/content/full/jcb.200606043/DC1), as previously described (Muller et al., 2002). More importantly, we observed strong up-regulation of Fhl2 in α-SMA–positive mesenchymal cells of wounded skin (Fig. 1 A). A series of five different tissue specimens obtained 5–14 d after wounding were analyzed by Fhl2 immunostaining. In all cases, we observed very strong signals present in the cytoplasm and the nucleus of myofibroblast-like cells of the granulation tissue, but not in differentiated fibroblasts from normal skin (Fig. 1 A). The myofibroblasts are characterized by α-SMA and SM22 immunoreactivity and, importantly, double-immunostainings of tissue sections for both Fhl2 (Fig. 1 B, red stain) and α-SMA or SM22 (Fig. 1 B, brown stain) indicated that the most abundant site of Fhl2 expression in the granulation tissue are indeed myofibroblasts. In contrast, keratinocytes did not reveal any Fhl2 immunoreactivity. These results, along with data obtained from human skin biopsies in vivo and from serum stimulation of cell lines, indicated that Fhl2 is up-regulated in myofibroblasts during wound healing and that it shuttles into the nucleus in response to exposure to bioactive lipids present in blood, as previously described (Muller et al., 2002; Morlon and Sassone-Corsi, 2003; Philippar et al., 2004).

We applied punch biopsy wounds to skin and cutaneous muscle of wild-type (*Fhl2*$^{+/+}$) and *Fhl2*-deficient (*Fhl2*$^{-/-}$) mice and conclusively found significant up-regulation of both Fhl2 mRNA and protein expression in *Fhl2*$^{+/+}$ mice during skin regeneration, with a maximum at 5 d after wounding (Fig. 2, A and B). In contrast, *Fhl2*$^{-/-}$ mice lack *Fhl2* mRNA and protein expression (Fig. 2, A and B). Intermediate levels of Fhl2 were induced in wounds of mice carrying a SM22 promoter-driven Fhl2 transgene in a *Fhl2*$^{-/-}$ genetic background (*Fhl2*$^{-/-}$*tgSM22Fhl2*). Interestingly, *Fhl2*$^{-/-}$ mice revealed severely impaired wound healing because only 10% of skin wounds were closed after 5 d, compared with 40% in *Fhl2*$^{+/+}$ mice (Fig. 2 C). After 12 d, all wounds of *Fhl2*$^{+/+}$ mice were closed, whereas only 80% were closed in *Fhl2*$^{-/-}$ mice. Importantly, the *Fhl2*$^{-/-}$*tgSM22Fhl2* transgenic mice that express intermediate Fhl2 mRNA and protein levels in a *Fhl2*$^{-/-}$ genetic background, displayed a nearly wild-type phenotype, with 30 and 90% wound closure at days 5 and 12, respectively, demonstrating rescue of the wound closure phenotype of *Fhl2*$^{-/-}$ mice. The same *SM22Fhl2* transgene expressed in a *Fhl2*$^{+/+}$ background, however, did not influence wound healing, indicating that the high levels of Fhl2 expression in *Fhl2*$^{+/+}$ mice are both necessary and sufficient for efficient wound healing. At each time point, 38–42 lesions were evaluated by measuring wound closure macroscopically, as well as by histological and immunochemical staining of skin sections. Collectively, our data indicate that the efficiency of wound closure correlates with the amount of Fhl2 mRNA and protein expression in wounds.

Fibroblasts play a key role in the formation of mechanical forces that lead to wound contraction, which is required to bring the wound margins together. Therefore, we were interested in

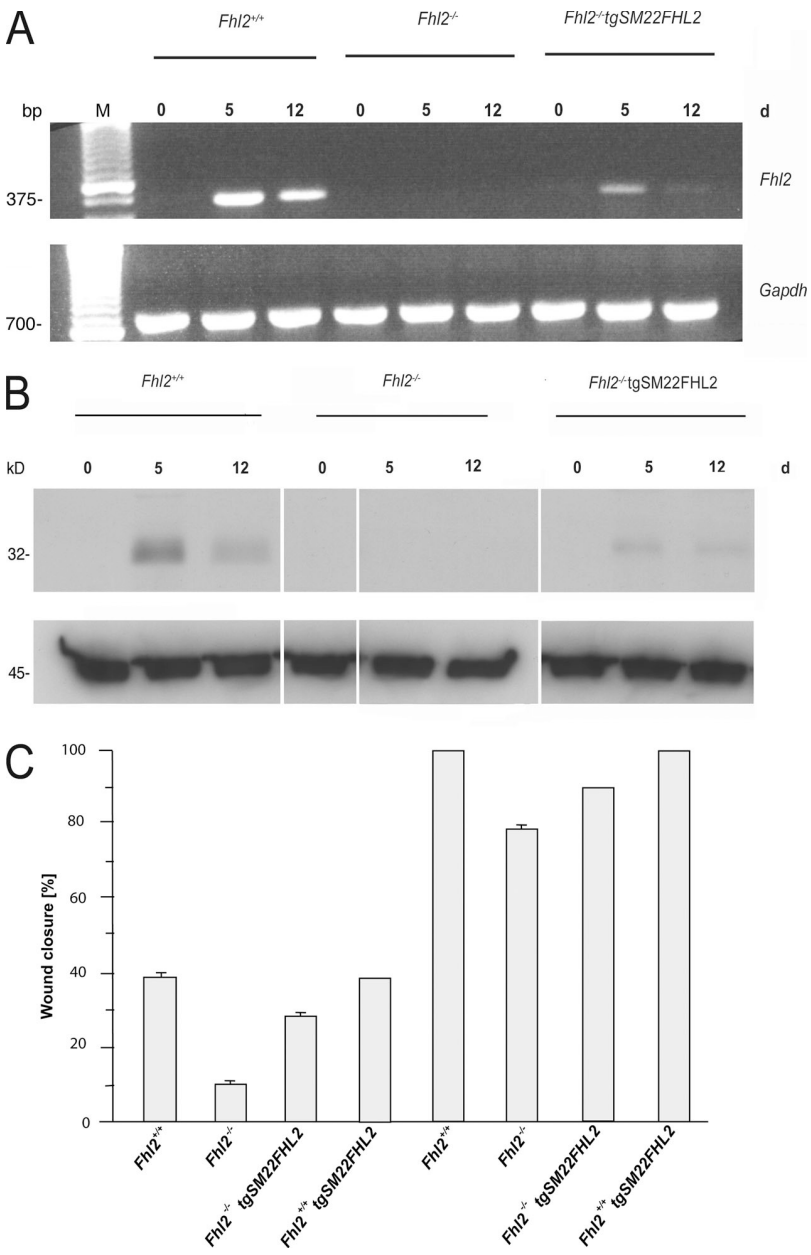

Figure 2. **Delayed wound healing in *Fhl2*$^{-/-}$ mice.** Up-regulation of *Fhl2* mRNA (A) and Fhl2 protein (B) in skin wounds 5 and 12 d after applying punch biopsies in Northern and Western blots, respectively. *Fhl2*$^{+/+}$ mice, *Fhl2*$^{-/-}$ mice (*Fhl2*$^{-/-}$), and the rescue mouse strain carrying a SM22-promoter Fhl2 transgene in an *Fhl2*$^{-/-}$genetic background (*Fhl2*$^{-/-}$*tgSM22Fhl2*) were used. *Gapdh* and β-actin served as loading controls. (C) Percentage of entirely closed wounds in *Fhl2*$^{+/+}$, *Fhl2*$^{-/-}$, *Fhl2*$^{-/-}$-rescue, and *Fhl2*$^{+/+}$*tgSM22Fhl2* mice after 5 and 12 d, respectively. 38–42 wounds for each genotype and time point were monitored by macroscopic inspection, and punch biopsies were verified histologically. Error bars represent the SD.

correlating the Fhl2 function with extracellular matrix remodeling and contraction. We analyzed the fibroblast-mediated contraction of type I collagen gels as an in vitro model of tissue remodeling. Fibroblasts derived from *Fhl2*$^{-/-}$ mice displayed a severe defect in collagen contraction, with a half-maximal contraction time of >60 h, compared with 10.4 h in *Fhl2*$^{+/+}$ cells (Fig. 3 A). The contraction of a collagen matrix was, in fact, so severely impaired in *Fhl2*$^{-/-}$ cells that we were unable to measure exactly the half-maximal contraction time within the observation interval. Because bioactive lipids stimulate fibroblast-mediated collagen contraction (Yanase et al., 2000), we analyzed collagen contraction in the presence of S1P. This resulted in a decreased half-maximal contraction time of 8.6 h for *Fhl2*$^{+/+}$ fibroblasts (Fig. 3 A). In contrast, S1P did not stimulate collagen contraction mediated by *Fhl2*$^{-/-}$ fibroblasts. Importantly, ectopic expression of Fhl2 in *Fhl2*$^{-/-}$ fibroblasts by transfection of an appropriate expression plasmid fully restored the capability to contract collagen (Fig. 3 A), demonstrating that Fhl2 is an essential component in this tissue remodeling assay.

During wound healing, mesenchymal cells differentiate upon stimulation by inflammatory cytokines into myofibroblasts, which produce high amounts of α-SMA and are involved in wound contraction in vivo (Hinz and Gabbiani, 2003). The early phase of wound healing is triggered by serum components released from injured blood vessels and degranulating platelets (Yatomi et al., 2000), which activate the transcription factor SRF (Chai and Tarnawski, 2002). SRF and Fhl2 interact physically (Philippar et al., 2004) and bind to the promoter of the SRF-responsive α-SMA gene. Degranulating platelets release large amounts of bioactive lipids, including S1P and lysophosphatidic acid, into wounds that, in turn, trigger nuclear translocation of Fhl2 (Muller et al., 2002). Therefore, we addressed

the question of whether Fhl2 may function as a transcriptional cofactor of SRF in activating α-SMA expression during wound healing.

For these assays, we tested cells of different origin (epithelial human embryonic kidney [HEK] 293 cells, mesenchymal stem cells, and fibroblasts), which are devoid of endogenous Fhl2 expression or with a Fhl2 knockout genotype, respectively. These cells were cotransfected with SRF- and Fhl2-expression constructs, together with a reporter plasmid carrying an α-SMA promoter-driven luciferase gene. Although expression of Fhl2 in HEK293 alone did not change reporter activity, we observed between two- and threefold activation in the mesenchymal cells (Fig. 3 B). SRF mediated an approximately fourfold increase of reporter expression in all cell lines. Importantly, expression of both SRF and Fhl2 resulted in approximately two- or threefold higher reporter activity than expression of SRF alone (Fig. 3 B), indicating coactivation of SRF-mediated transcriptional activity in all three cell lines.

We characterized α-SMA expression in myofibroblasts during wound healing in *Fhl2*$^{-/-}$ and *Fhl2*$^{+/+}$ mice. As expected, immunohistochemical staining revealed strong expression of α-SMA in myofibroblasts of the granulation tissue

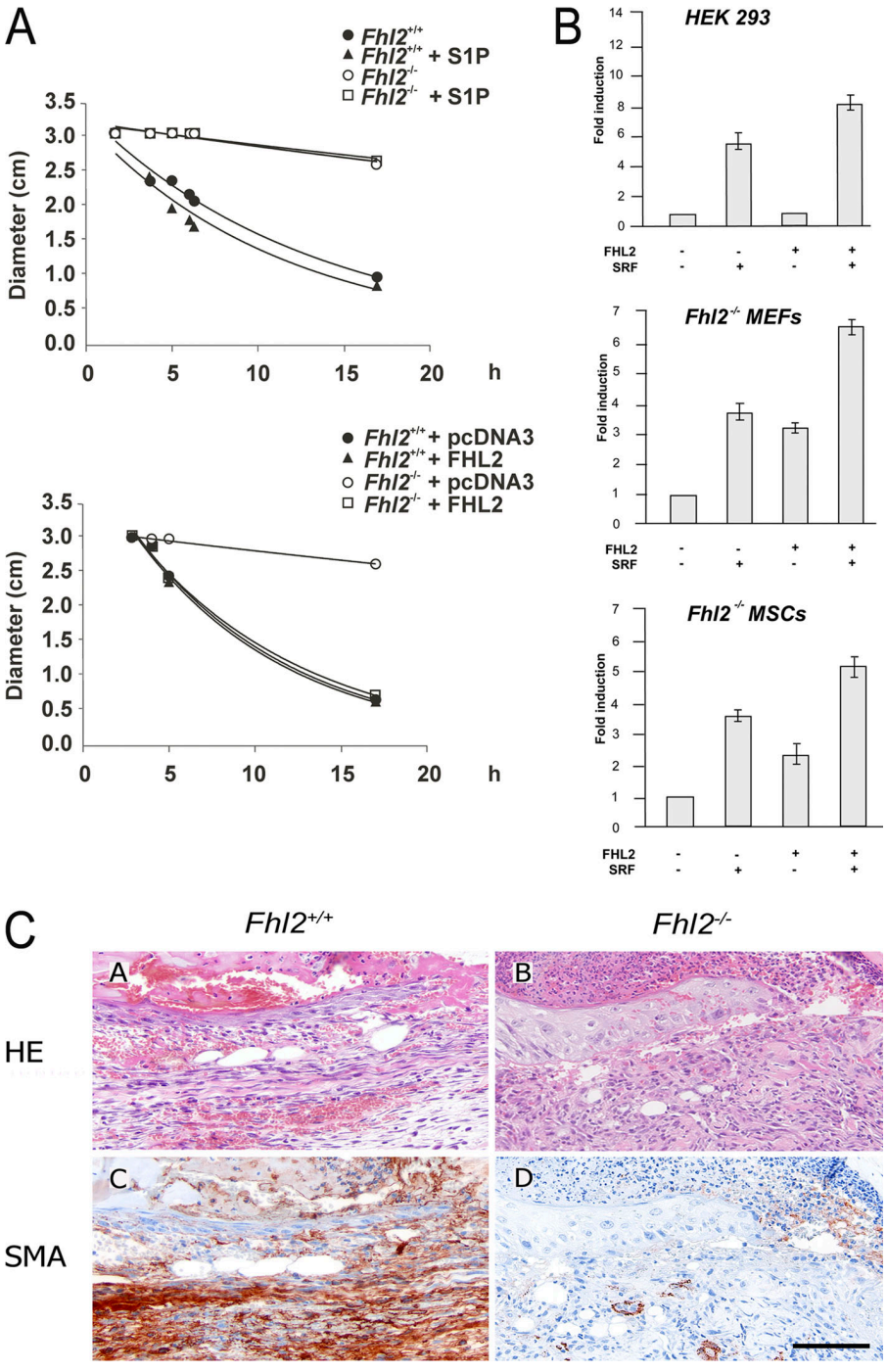

Figure 3. **Fhl2 regulates fibroblast contractility and coactivates SRF-mediated α-SMA transcription in wound healing.** (A) Defective collagen contraction in *Fhl2*$^{-/-}$ embryonic fibroblasts (top). Collagen contraction and stimulation in response to treatment with S1P were restored after retransfecting Fhl2 cDNA into *Fhl2*$^{-/-}$ fibroblasts (bottom). Transfections were done in triplicate, with either empty vector (pcDNA3) or Fhl2 expression plasmid (Fhl2). SDs were <2% in all cases. (B) HEK293, *Fhl2*$^{-/-}$ fibroblasts (MEFs), and *Fhl2*$^{-/-}$ mesenchymal stem cells (MSCs) were transfected with an α-SMA promoter-driven luciferase reporter construct and expression plasmids for SRF and Fhl2. Bars indicate the fold induction of transfecting SRF, Fhl2, and both expression vectors versus the luciferase activity of the reporter plasmid. $n = 3$. Error bars represent the SD. (C) Cutaneous lesions 5 d after applying skin punch wounds to *Fhl2*$^{+/+}$ and *Fhl2*$^{-/-}$ mice. Images show hematoxylin and eosin staining (HE, top) and immunohistochemical stainings for α-SMA expression (bottom). There is strong α-SMA reactivity in the granulation tissue of *Fhl2*$^{+/+}$, but not of *Fhl2*$^{-/-}$, mice below the reepithelializing keratinocytes on top. Bar, 100 μm.

below the wound surface at day 5 in *Fhl2*$^{+/+}$ mice, but only very weak signals in knockout animals (Fig. 3 C). Systematically scoring the intensity of α-SMA staining in 100 fibroblasts below every wound surface revealed significantly weaker staining in *Fhl2*$^{-/-}$ mice (relative units, 1.25 ± 0.6 at day 5 and 1.4 ± 1.0 at day 12, respectively) than in *Fhl2*$^{+/+}$ mice (relative units, 2.6 ± 0.75 at day 5 and 2.0 ± 0.6 at day 12, respectively). The difference in α-SMA staining intensity was that it was statistically significant at day 5 ($P < 0.001$) and was still significant at day 12 ($P < 0.1$). Importantly, immunostainings of the transgenic *SM22Fhl2* rescue mouse strain did not reveal any difference in α-SMA reactivity compared with *Fhl2*$^{+/+}$ mice. These results indicate that activation of α-SMA expression in myofibroblasts and wound closure occurred less efficiently and slower in *Fhl2*$^{-/-}$ mice.

Cutaneous wound healing is inevitably associated with migration of mesenchymal precursor cells and their subsequent differentiation into myofibroblasts. Within the first days after wounding, mesenchymal cells invade the wound to replace the clot and to form a granulation tissue. To address the question of whether Fhl2 influences the migration capacity of such cells, we established mesenchymal stem cell lines from bone marrow of *Fhl2*$^{+/+}$ and *Fhl2*$^{-/-}$ mice (Fig. 4 A). The morphology of different Fhl2$^{-/-}$ clones was quite similar, but differed from that of Fhl2$^{+/+}$ clones. *Fhl2*$^{-/-}$ cells showed a more epithelial-like form and had a less polar shape, often with many short actin stress fibers running in different directions. *Fhl2*$^{+/+}$ cells had a more fibroblast-like form, with many filopodial and lamellipodial structures. They displayed a well-organized actin cytoskeleton with long microfilament cables running across the whole cell body (Fig. 4 A), and Fhl2 was localized at focal adhesion structures, as well as along the actin filaments. Analysis of the migration capacity revealed a motility defect of *Fhl2*$^{-/-}$ cells (Fig. 4 B and Videos 1 and 2, available at http://www.jcb.org/cgi/content/full/jcb.200606043/DC1). *Fhl2*$^{-/-}$ cells showed much less activity in the formation of filopodia or lamellipodia and, consequently, needed almost twice as much time to close a cell-free cleft in comparison with *Fhl2*$^{+/+}$ cells. (Fig. 4 B and Videos 1 and 2). Importantly, ectopic expression of a myc-tagged Fhl2 protein (Fig. S2 A) rescued the impaired migration

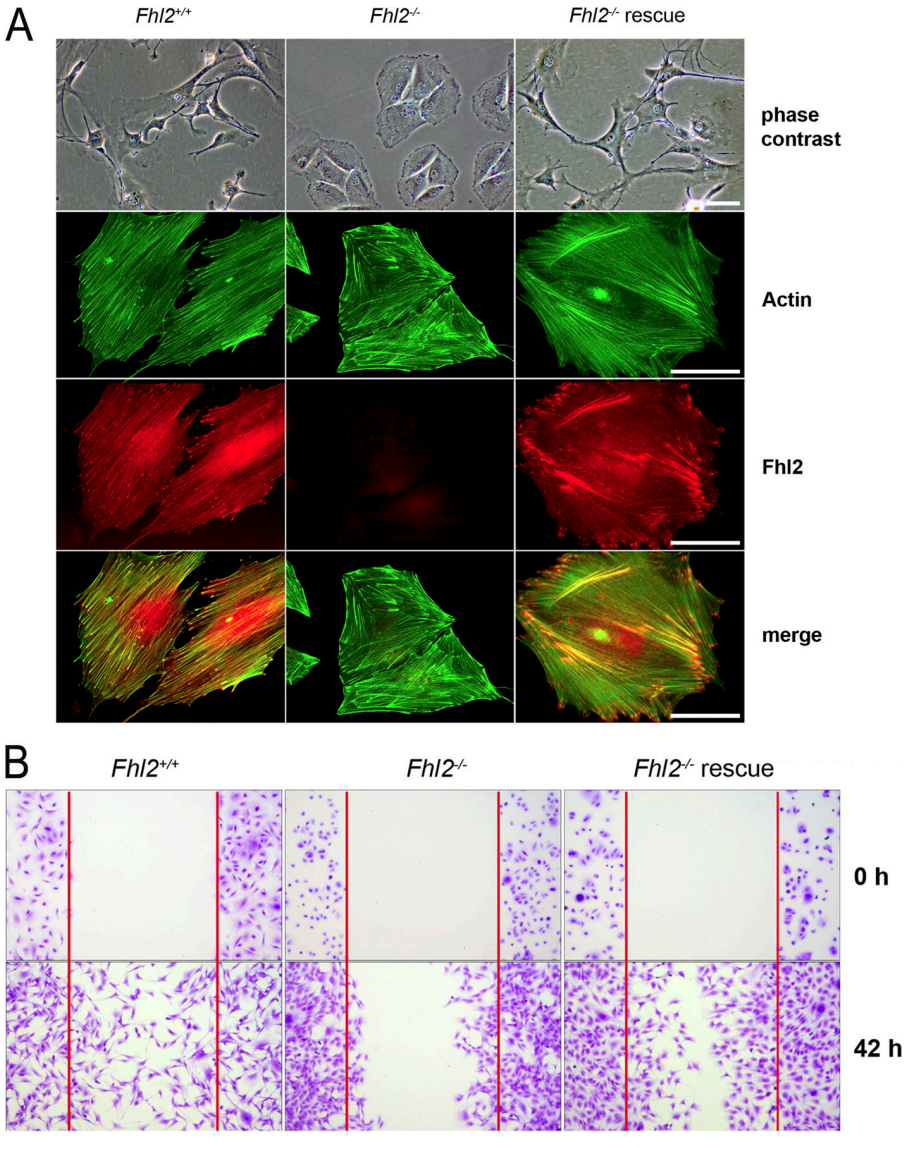

Figure 4. **Reduced motility of *Fhl2*$^{-/-}$ mesenchymal stem cells.** (A) *Fhl2*$^{+/+}$, *Fhl2*$^{-/-}$, and *Fhl2*$^{-/-}$-rescue stem cells were examined regarding shape (top), actin cytoskeleton organization, and distribution of Fhl2 protein (bottom). F-actin was visualized with Alexa Fluor 488–coupled phalloidin (green). *Fhl2*$^{+/+}$ and *Fhl2*$^{-/-}$ cells were immunostained for Fhl2 with the F4B2 monoclonal antibody, *Fhl2*$^{-/-}$ rescued cells with the anti-myc 9E10 monoclonal antibody. Bars, ∼50 μm. (B) Migration of *Fhl2*$^{+/+}$, *Fhl2*$^{-/-}$, and *Fhl2*$^{-/-}$-rescue mesenchymal stem cells. Cell migration on uncoated dishes into cell-free areas was photographed at 0 and 42 h.

activity of the *Fhl2*$^{-/-}$ cells (Fig. 4 B and Video 3). The ectopic expression of Fhl2 not only rescued the motility phenotype but also reverted the cell shape and actin cytoskeleton organization to that of *Fhl2*$^{+/+}$ stem cells (Fig. 4 A). Impaired cell motility was independent of the substrate on which the cells migrated (fibronectin, laminin-1, or no substrate) and of the cell origin. On uncoated dishes, cell movement was slower, with 10.8 ± 1.4 μm/h for *Fhl2*$^{+/+}$, 5.8 ± 0.9 μm/h for *Fhl2*$^{-/-}$, and 9.6 ± 0.9 μm/h for rescued mesenchymal stem cells. On fibronectin-coated dishes, the migration velocity was 17.1 ± 0.7 μm/h for *Fhl2*$^{+/+}$, 8.8 ± 0.4 μm/h for *Fhl2*$^{-/-}$, and 12.0 ± 1.5 μm/h for *Fhl2*$^{-/-}$-rescued cells, respectively. The diminished migratory activity of *Fhl2*$^{-/-}$ cells was not caused by changes of the integrin pattern on their surface, as *Fhl2*$^{+/+}$, *Fhl2*$^{-/-}$, and rescued cells all expressed equal amounts of integrin β1–containing receptors (Fig. S2 B). Like *Fhl2*$^{+/+}$ cells, the *Fhl2*$^{-/-}$ or rescued cells attached equally well to proteins of the extracellular matrix, suggesting that different adhesion properties are not responsible for the reduced migratory capacity.

Interestingly, the impaired cell migration and the cytoskeletal changes of *Fhl2*$^{-/-}$ cells remarkably resemble the phenotype of FAK-deficient cells (Ilic et al., 1995). In addition, it is known that FAK has to be activated for cell migration (Mitra et al., 2005). After adhesion to extracellular matrix molecules, FAK is autophosphorylated at tyrosine Y397, recruiting Src, which in turn phosphorylates FAK at additional Y residues, including Y861, which serves as the binding site for p130Cas. Interaction of p130Cas and FAK leads to recruitment of multiple other proteins, finally resulting in the formation of lamellipodia and cell migration (Playford and Schaller, 2004; Mitra et al., 2005). Analysis of FAK tyrosine phosphorylation showed that the overall phosphorylation pattern was identical in *Fhl2*$^{+/+}$, *Fhl2*$^{-/-}$, and *Fhl2*$^{-/-}$-rescued mesenchymal cell lines (Fig S3, available at http://www.jcb.org/cgi/content/full/jcb.200606043/DC1). Only pY861, serving as the binding site for p130Cas, was slightly hyperphosphorylated in the *Fhl2*$^{-/-}$ cells. We previously showed that Fhl2 directly binds to integrins (Wixler et al., 2000) and FAK (Gabriel et al., 2004), and that it is localized at

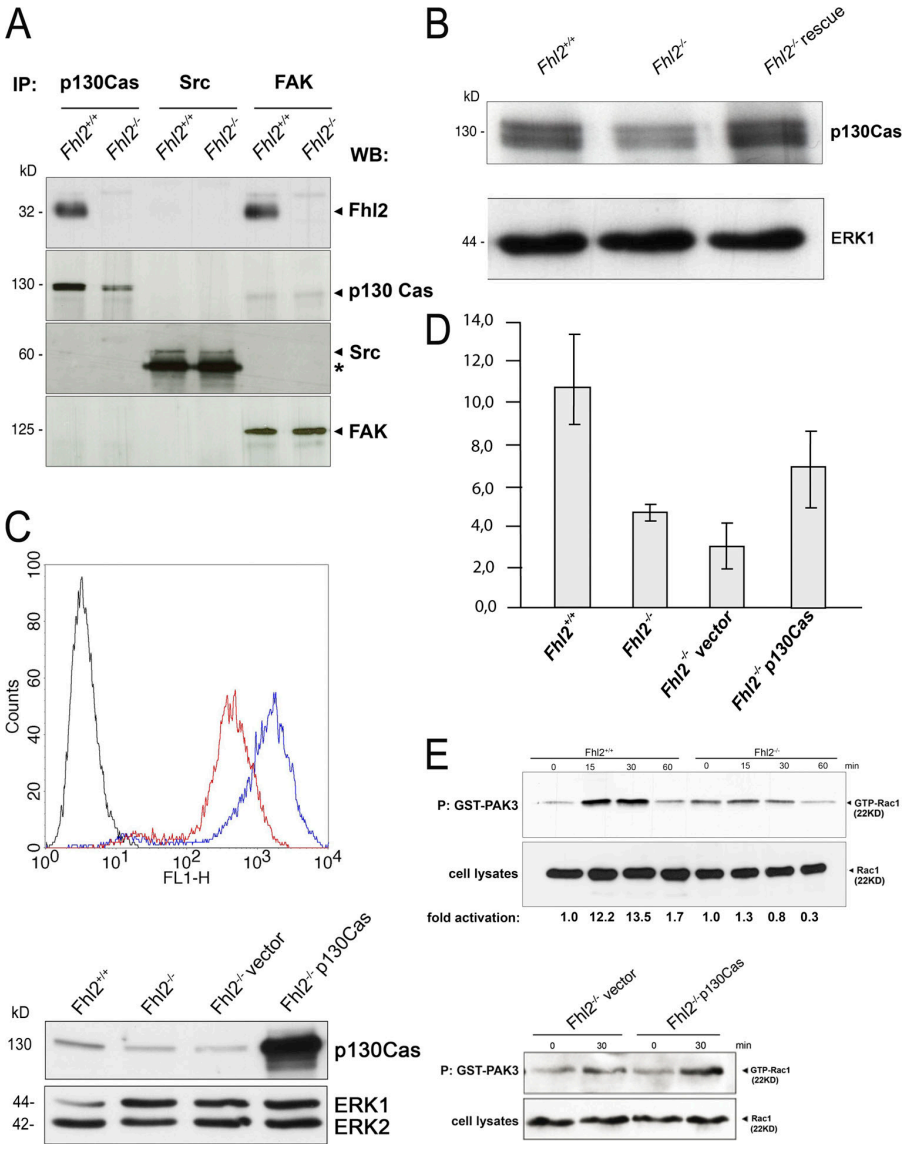

Figure 5. **Reduction of p130Cas expression in *Fhl2*$^{-/-}$ cells.** (A) p130Cas, Src, or FAK proteins were immunoprecipitated from lysates of fibronectin-stimulated *Fhl2*$^{+/+}$ or *Fhl2*$^{-/-}$ cells and analyzed by immunoprobing for the proteins indicated. (B) Recombinant expression of myc-Fhl2 in *Fhl2*$^{-/-}$ cells reverses p130Cas expression. Immunoblot with anti-ERK1 antibody served as loading controls. 10 μg of total cell lysates were analyzed. (C) Expression control of p130Cas in *Fhl2*$^{-/-}$ stem cells. Cells were infected with retroviruses containing the GFP vector or GFP+p130Cas. 48 h later the cells were harvested and one part was used for analysis of infection efficiency by FACScan (top) or by immunoblotting (bottom). Black curve of the FACScan profile, noninfected cells; blue curve, GFP-vector–infected cells; red curve, GFP+p130Cas–infected cells. For immunoblotting, 7.5 μg of total cell lysates were separated on 10% SDS-PAGE, and p130Cas and ERK1/2 (as loading controls) were detected with specific antibodies. (D) The second part of infected cells, along with noninfected *Fhl2*$^{+/+}$ and *Fhl2*$^{-/-}$ cells, was used for migration assays. Migration of cells on noncoated or on fibronectin-precoated dishes was studied. The assays were performed twice with similar results. Only cell motility on noncoated dishes is shown. Error bars represent the SD. (E) Reduction of Rac activation in *Fhl2*$^{-/-}$ cells (top) and increased Rac activation in p130Cas-overexpressing *Fhl2*$^{-/-}$ cells (bottom). The cells were serum-starved overnight, trypsinized, and plated for 15, 30, and 60 min on cell culture dishes precoated with 20 μg/ml fibronectin. For precipitation of GTP-loaded Rac, cells were lysed in Triton X-100 lysis buffer, and 400 μg of protein lysates were rotated with GST-PAK3–coated glutathione beads. The precipitates and the lysates were analyzed for the presence of Rac1 by SDS-PAGE and Western Blotting. The fold of Rac activation was estimated densitometrically as the relative intensity of the GTP-Rac bands to the loading controls. Values at time point 0 were taken as unity.

focal adhesion sites (Samson et al., 2004). Analysis of immunocomplexes from lysates of *Fhl2*$^{+/+}$ and *Fhl2*$^{-/-}$ cells showed that Fhl2 coimmunoprecipitated with FAK and p130Cas, but not with Src, when cells were plated on fibronectin-coated dishes (Fig. 5 A). Interestingly, the level of p130Cas was significantly reduced in *Fhl2*$^{-/-}$ cells, whereas the amounts of FAK and Src were not altered (Fig. 5 A). Furthermore, as shown in Fig. 5 B, the level of p130Cas was similar to that of *Fhl2*$^{+/+}$ cells when the Fhl2 protein was reexpressed in *Fhl2*$^{-/-}$ cells.

Next, quantitative real-time PCR experiments were performed to study whether the changes in p130Cas expression levels result from differences in mRNA expression. Amplification curves for p130Cas and, as a reference gene, cyclophilin, were obtained with template cDNA from Fhl2$^{+/+}$ and Fhl2$^{-/-}$ mesenchymal stem cells. Each curve shown in the Fig. S4 A (available at http://www.jcb.org/cgi/content/full/jcb.200606043/DC1) represents the mean of three replicates from a single cDNA sample. The amplification of p130Cas cDNA was delayed in Fhl2$^{-/-}$ cells compared with *Fhl2*$^{+/+}$ cells, indicating a lower p130Cas mRNA amount. The difference between the average Ct-value of p130Cas and cyclophilin (ΔCt) was calculated for both cell lines. These values were compared (ΔΔCt), and the relative amount of p130Cas mRNA was calculated ($2^{-\Delta\Delta Ct}$) and diagrammed (Fig. S4 B). In summary, our data clearly indicate that Fhl2 knockout cells express roughly twofold lower p130Cas mRNA levels.

Recruitment of p130Cas subsequently leads to activation of Rac and cell migration (Playford and Schaller, 2004; Mitra et al., 2005). Therefore, we asked whether expression of p130Cas in *Fhl2*$^{-/-}$ mesenchymal stem cells would be able to rescue the defect in cell migration. Knockout stem cells were infected with retroviruses expressing either p130Cas along with GFP or GFP alone as a control. The p130Cas and GFP genes were connected by an internal ribosomal entry-site sequence. Evaluation of GFP-labeled cells indicated that the infection efficiency was 94.1 and 95.2%, respectively (Fig. 5 C, left). Consistently, Western blots indicated robust expression of p130Cas in the knockout cells (Fig. 5 C, right). Analysis of cell motility revealed that the migratory capacity of Fhl2$^{-/-}$ cells that overexpressed p130Cas was enhanced in comparison with *Fhl2*$^{-/-}$ cells, but did not reach the velocity of *Fhl2*$^{+/+}$ cells. These results were obtained independently of whether cells migrated on noncoated or on fibronectin-coated surfaces (Fig. 5 D). Thus, reexpression of p130Cas rescued the migratory phenotype of *Fhl2*$^{-/-}$ cells, but not entirely to the level of *Fhl2*$^{+/+}$ cells.

Finally, we asked whether changes in expression of p130Cas resulted in different levels of Rac activation. Therefore, *Fhl2*$^{+/+}$, knockout, and *Fhl2*$^{-/-}$ cells stably expressing p130Cas or the empty vector were assayed for Rac activity. The cells were serum-starved overnight, trypsinized, and plated for 15, 30, or 60 min, respectively, on cell culture dishes precoated with 20 mg/ml fibronectin. For precipitation of GTP-loaded Rac, cells were lysed in Triton X-100 lysis buffer, and 400 mg protein were rotated with GST-PAK3–coated glutathione beads. Although the activation kinetics slightly varied in separate experiments, a reproducible difference in the Rac activation between *Fhl2*$^{+/+}$ and *Fhl2*$^{-/-}$ cells was observed. Data shown in Fig. 5 E clearly indicate that knockout cells activate Rac less efficiently than *Fhl2*$^{+/+}$ cells, and that *Fhl2*$^{-/-}$ cells reconstituted with p130Cas restore their capability to activate Rac in response to attachment to fibronectin.

Discussion

Previous studies, mainly based on cell lines in vitro, established Fhl2 as a serum-responsible signal transducer shuttling in response to SP1 and lysophosphatidic acid from the cell membrane into the nucleus, where it functions as a nuclear coactivator of transcription factors. However, only few transcriptional targets, including Fhl2 itself, were described, and the function of Fhl2 signaling in vivo is much less explored. Although a function of Fhl2 in promoting differentiation of myoblasts was suggested (Martin et al., 2002), Fhl2 knockout mice developed only a mild phenotype with bone formation defects and an increased sensitivity in respect to a hypertrophic response to β-adrenergic stimulation in the heart (Kong et al., 2001; Bai et al., 2005; Gunther et al., 2005; Lai et al., 2006).

Data presented in our study indicate that Fhl2 further mediates nonredundant signaling during wound healing. *Fhl2*$^{-/-}$ mice clearly revealed delayed wound healing, reduced migration of mesenchymal precursor cells, delayed activation of α-SMA, and impaired wound contraction. The Fhl2 protein is activated in dermal fibroblasts after release of bioactive lipids in wounded tissue and, indeed, we show that Fhl2 regulates the expression of α-SMA by coactivation of SRF, and thereby the contractility of the granulation tissue. Therefore, it seems that nuclear shuttling and transcriptional coactivation of Fhl2 developed as a signaling pathway mediating rapid adaptation of cells and tissues in response to pathological stress conditions. Our data further indicate that Fhl2 signaling is cell-type specific and different from its function in cardiac muscle cells, where it negatively regulates expression of SMA (Philippar et al., 2004).

In addition, Fhl2 interacts with proteins of focal adhesion structures at the membrane or cytosolic level, and we provide first evidence that because of this interaction Fhl2 regulates cell motility and contractility. Contraction of the granulation tissue facilitates wound closure by bringing the wound margins together. Efficient contraction of myofibroblasts requires a well-developed cytoskeleton, which is established by expression of α-SMA and its incorporation into actin stress fibers (Hinz and Gabbiani, 2003). Hence, expression of α-SMA by skin fibroblasts is a critical step in wound healing. Interestingly, our data for the first time provide a mechanistic link between release of the bioactive lipids S1P and lysophosphatidic acid from platelets during clotting and wound healing and the contractile activity of the granulation tissue. These substances trigger, in a Rho-dependent manner, nuclear shuttling of Fhl2 (Muller et al., 2002) where it acts as a coactivator of α-SMA transcription. Consistent with these data, we further demonstrated that in the absence of Fhl2, the contractile forces of fibroblasts are dramatically reduced and that this defect can be rescued by expression of exogenous Fhl2 protein.

It is well known that FAK plays a key role in cell migration. It is activated upon integrin engagement and recruits several

cytosolic proteins that drive cell migration. We show that the expression of the downstream signaling molecule p130Cas, which regulates the activity of the Rac GTPase, and hence, cell migration, is down-regulated in *Fhl2*$^{-/-}$ cells. Our data, however, also indicate that the mechanism by which Fhl2 regulates cell migration is more complex and cannot be reduced just to the level of p130Cas protein, as its overexpression did not restore migration velocity of mesenchymal cells to the full level of *Fhl2*$^{+/+}$ cells. Thus, it appears that Fhl2 activation in mesenchymal cells after wounding regulates different effector functions of activated FAK. A separate study of our group provided evidence that Fhl2 is also involved in organization of focal adhesion structures and in regulation of matrix assembly (unpublished data).

In summary, we show for the first time that *Fhl2*$^{-/-}$ mice display a cutaneous wound-healing phenotype that can be rescued by ectopic expression of Fhl2. Our data demonstrate reduced expression of α-SMA and p130Cas and, subsequently, less efficient activation of Rac in *Fhl2*$^{-/-}$ cells, which lead to severe defects in collagen contraction and migration. Thus, lipid-triggered Fhl2 signaling is mechanistically involved in regulating wound healing and may represent a new therapeutic target.

Materials and methods

Fhl2$^{-/-}$ and transgenic mice

Fhl2$^{-/-}$ mice were provided by R. Bassel-Duby (University of Texas Southwestern Medical Center, Dallas, TX) and published previously (Kong et al., 2001). For the generation of transgenic mice, the human Fhl2 cDNA was coupled with a 1.4-kb SM22α promoter (Jain et al., 1998) and animals were obtained according to published procedures (Jager et al., 2003). Genotyping was done by PCR analysis from tail genomic DNA using the primer pairs 5′-GACTGCTCCAACTTGGTGTCTTTC-3′ and 5′-TCCCGCAGGATGTACTTCTTGC-3′ in 35 amplification cycles (95°C for 30 s, 54°C for 30 s, and 72°C for 30 s). All animals were maintained in a pure C57BL/6 background, and subpairs were used for the wounding experiments.

Wound-healing experiments

48 6-wk-old mice (18 *Fhl2*$^{+/+}$, 18 *Fhl2*$^{-/-}$, and 12 transgenic mice) were used. 2–4 0.6-cm punch wounds, including the skin and cutaneous muscle, were cut into each mouse and left to heal by secondary intention, essentially as previously described (Ashcroft et al., 1999). At days 0, 5, and 12, wounds were dissected and paraffin-embedded for histology or snap-frozen in liquid nitrogen for RNA and protein extraction. All experiments were performed in compliance with animal welfare regulations (Permission No. 50.203.2-BN12, 12/02 by the Regierungspräsidium, Cologne, Germany).

Cell culture and collagen contraction assays

Mouse embryonal fibroblasts were obtained by standard procedures and maintained in DME (Invitrogen) supplemented with 100 U/ml penicillin, 10 μg/ml streptomycin, and 10% FCS (Invitrogen). Transient transfection of fibroblasts was done using the Amaxa system (Amaxa) with transfection efficiency >50% measured by GFP expression (Hamm et al., 2002). Collagen contraction was performed as previously described (Bell et al., 1979; Grinnell, 2000). In brief, 250 μl of fibroblast suspension (10^6 cells/ml) were added to 3 ml collagen type I solution (3 mg/ml) and placed into a 30-mm Petri dish (Greiner). Contraction of the developing collagen sponge was determined by measuring the diameter every 1 h.

Mesenchymal stem cells were derived from bone marrow cells of 4-wk-old C57BL/6 *Fhl2*$^{+/+}$ or *Fhl2*$^{-/-}$ mice as previously published (Park et al., 2006). The expanded cells had a doubling time of ∼35 h and were positive for CD34, c-kit, sca1, Thy1, and CD13, and negative for CD45, CD10, and CD31 marker as determined by PCR. According to these markers and to their potency to differentiate into osteogenic, chondrogenic, and adipogenic lineages, we identified them as mesenchymal cell lineages. The cells were maintained in a mixture of DMEM and MCDB-201 medium supplemented with 2% FCS, 10 ng/ml EGF (Sigma-Aldrich), 10 ng/ml PDGF (R&D Systems), 1,000 U/ml of mouse LIF (CHEMICON International, Inc.), 1× insulin–transferrin–selenium mixture (Sigma-Aldrich), and 10^{-9}M dexamethasone (Sigma-Aldrich). The *Fhl2*$^{-/-}$ rescue cells were obtained by infection of *Fhl2*$^{-/-}$ cells with retroviruses containing a myc-tagged human Fhl2, as we previously described (Samson et al., 2004).

Northern and Western blots

Total cellular RNA was extracted from harvested cells or homogenized wound specimens by lysis in guanidinium isothiocyanate. 10 μg was separated by electrophoresis in a 1.2% agarose/formaldehyde gel, transferred to a nylon membrane (Hybond N$^+$; GE Healthcare), and probed with radiolabeled *Fhl2* cDNA. Soluble protein lysates were extracted from cells or homogenized wound specimens in 150 mM NaCl, 10 mM Tris, pH 7.2, 0.1% SDS, 1% Triton X-100, and 1% deoxycholate and 5 mM EDTA and centrifuged at 13,000 *g* for 20 min at 4°C. 15 μg of protein lysates were denatured at 90°C for 10 min, run on 12% SDS-PAGE gels, and electroblotted to a PVDF membrane (Roti-PVDF; Roth GmbH) using standard protocols. After blocking in 5% nonfat dry milk/PBST for 2 h, the membranes were incubated for 1 h with a monoclonal anti-Fhl2 antibody (dilution 1:2,000), washed, incubated with horseradish peroxidase–conjugated secondary antibody (dilution 1:1,000; DakoCytomation), and developed using ECL chemiluminescence (GE Healthcare). As a control, blots were probed with a primary anti–β-Actin antibody (dilution 1:5,000; DakoCytomation). Images were captured on film, digitized, and if needed, minor linear adjustments in contrast were made using Photoshop software (Adobe).

Quantitative real-time PCR

Total RNA was extracted with the RNeasy kit (QIAGEN) from two independent samples of Fhl2$^{+/+}$ and Fhl2$^{-/-}$ stem cells, respectively. Reverse transcription of RNA (1.5 μg) was performed with oligo(dT) primers and RevertAid H Minus M-MuLV reverse transcriptase (Fermentas MBI). For PCR amplification of cDNA, specific primers (MWG) were used to detect differences in the expression levels of p130Cas; primers for murine p130Cas were chosen according to Jayanthi et al. (2002). Primers for the reference gene cyclophilin were as follows: 5′-CCACCGTGTTCTTCGACAT-3′ (upstream) and 5′-CAGTGCTCAGAGCTCGAAAG-3′ (downstream). The PCR reactions were done in triplicate for each cDNA after the Stratagene protocol with 2× Brilliant SYBR Green QPCR Master Mix (Stratagene), with preheating at 95°C for 10 min; 40 cycles of 95°C for 30 s, 60°C for 1 min, and 72°C for 30 s; and 95°C for 1 min, 60°C for 30 s, and 95°C for 30 s. MxPro Software (Stratagene) was used for analysis.

Immunostainings and acquisition of images

4-μm tissue slides were cut from formalin-fixed and paraffin-embedded wound specimens and used for staining with hematoxylin and eosin or by immunohistochemistry. Indirect immunohistochemistry was done by the avidine-biotin method, as previously described (Friedrichs et al., 2005). Primary antibodies were anti–human α-SMA (1:25 dilution; DakoCytomation), anti-SM22 (1:100 dilution; DakoCytomation), anti–cytokeratin-5 (1:100 dilution; DakoCytomation), and anti–collagen type I (1:100 dilution; ICN Biochemicals). Slides were incubated with a secondary goat anti–mouse serum (dilution 1:200; DakoCytomation), reacted with the ABC kit (Vector Laboratories), and peroxidase activity was visualized with 3-amino-9-ethylcarbazole (Sigma-Aldrich). Double immunostaining with a second alkaline phosphatase–labeled antibody (DakoCytomation) was done as previously described (Friedrichs et al., 2005). Pictures were taken by using a light microscope DM LB2 (Leica) and the analysis system software Diskus (Hilgers).

For immunofluorescence staining, 5×10^5 fibroblasts were seeded in chamber slides (Nunc), grown to 75% confluency, and incubated for 48 h in medium containing 10 or 0.5% FCS. Indirect immunofluorescence staining was done as previously described (Muller et al., 2002), using rabbit anti-Fhl2 antibody (1:300), anti-Fhl2 mAb clone F4B2 (Samson et al., 2004), or anti-myc mAb derived from clone 9E10 (American Type Culture Collection). Cell images were taken using an Axiovert 2000 ApoTome microscope with an AxioCam digital camera and AxioVision software (Carl Zeiss MicroImaging, Inc.).

Cell transfections and luciferase assays

Transfections of 293 cells and luciferase assays were performed as previously described (Muller et al., 2002). 500 ng of the reporter plasmid pSM8pGL3 were cotransfected with expression plasmids coding for SRF

(2.5 ng) and Fhl2 (5 ng pCMX-Fhl2) as indicated. Transfections of *Fhl2*$^{-/-}$ fibroblasts were performed with Lipofectamine (Invitrogen), and transfections of *Fhl2*$^{-/-}$ stem cells were performed with Fugene 6 (Roche) as recommended by the manufacturers. Relative light units were normalized to protein concentration using the Bradford dye assay (Bio-Rad Laboratories). For construction of pSM8pGL3, the α-SMA promoter and the first intron (SMP8; a gift from E.P. Smith, University of Cincinnati College of Medicine, Cincinnati, OH) were cloned in pGL3 (Promega). SMP8 contains −1,074 bp of the 5′- flanking region, 63 bp of 5′-UT, and the 2.5-kb first intron of the α-SMA.

For generation of p130Cas retrovirus stocks, the cDNA of human p130Cas (a gift from K.H. Kirsch, Boston University Medical School, Boston, MA) was cloned into the bicistronic retroviral pEGZ vector before the internal ribosomal entry-site sequence and the GFP gene. After transfection of Phoenix virus-producer cells (Orbigen, Inc.) with pEGZ vector alone or pEGZ-p130Cas, the cells were selected for zeocin resistance, and supernatants from confluent monolayers were used as retroviral stocks.

Cell migration assay

Cell migration studies were performed essentially as previously described (Lavrovskii and Razvorotnev, 1976). In brief, 5×10^3 cells in 0.8 ml of DMEM with 10 ng/ml EGF and PDGF were plated onto 48-well plates, which were precoated with fibronectin, laminin-1, or nothing and blocked with 1% BSA. To produce a cell-free "window," 1-mm-thick steel plates were inserted into wells before seeding the cells and were removed again after the cells had been attached to the bottom. This method has the advantage over the frequently used "scratch window" assay in that the substrate in the window is not destroyed. The migration was monitored by inverted microscopy at the times indicated. For videos, the scratch assay was used.

Flow cytometry

10^5 cells were suspended in FACS-PBS (PBS containing 2% FCS and 0.02% NaN_3). Cells were incubated with integrin anti-β1 Abs (clone 9EG7; BD Biosciences) for 20 min on ice, washed twice with FACS-PBS, and incubated with Cy2-conjugated secondary antibodies (DakoCytomation) for additional 15 min. After washing the cells, measurements were performed with a FACSCalibur flow cytometer (BD Biosciences).

Statistics

For all statistical analyses, the Cochran-Armitage trend test was used and a P-value <0.05 was considered statistically significant. To quantify the α-SMA immunohistochemical staining results, the following scoring system was applied: no staining, 0; weak staining, 1; moderate staining, 2; maximal staining, 3. 100 cells of each sample were evaluated.

Online supplemental material

Fig. S1 shows that Fhl2 mRNA is serum-inducible in embryonic mouse fibroblasts and that Fhl2 translocates into the nucleus and along the actin cytoskeleton in response to FCS. Fig. S2 shows the migration activity of *Fhl2*$^{+/+}$, *Fhl2*$^{-/-}$, and rescued mesenchymal stem cells (Videos 1–3 are time-lapse movies correlating to Fig. S2). Fig. S3 shows that the absence of Fhl2 does not influence FAK autophosphorylation after adhesion of stem cells to fibronectin. Fig. S4 shows results from real-time qRT-PCR, indicating that Fhl2$^{-/-}$ cells express reduced levels of p130Cas mRNA. Online supplemental material is available at http://www.jcb.org/cgi/content/full/jcb.200606043/DC1.

We thank G. Klemm for excellent help with the artwork, A. Jacob for help with the animal experiments, and G. Gabbiani for helpful discussions.

This work was supported by grants from the Mildred-Scheel-Stiftung to V. Wixler, R. Schule, and R. Buettner, and from the German Research Foundation to V. Wixler., H. Schorle, and R. Buettner.

Submitted: 8 June 2006
Accepted: 11 March 2007

References

Ashcroft, G.S., X. Yang, A.B. Glick, M. Weinstein, J.L. Letterio, D.E. Mizel, M. Anzano, T. Greenwell-Wild, S.M. Wahl, C. Deng, and A.B. Roberts. 1999. Mice lacking Smad3 show accelerated wound healing and an impaired local inflammatory response. *Nat. Cell Biol.* 1:260–266.

Bai, S., H. Kitaura, H. Zhao, J. Chen, J.M. Muller, R. Schule, B. Darnay, D.V. Novack, F.P. Ross, and S.L. Teitelbaum. 2005. FHL2 inhibits the activated osteoclast in a TRAF6-dependent manner. *J. Clin. Invest.* 115:2742–2751.

Bell, E., B. Ivarsson, and C. Merrill. 1979. Production of a tissue-like structure by contraction of collagen lattices by human fibroblasts of different proliferative potential in vitro. *Proc. Natl. Acad. Sci. USA*. 76:1274–1278.

Chai, J., and A.S. Tarnawski. 2002. Serum response factor: discovery, biochemistry, biological roles and implications for tissue injury healing. *J. Physiol. Pharmacol.* 53:147–157.

Friedrichs, N., R. Jager, E. Paggen, C. Rudlowski, S. Merkelbach-Bruse, H. Schorle, and R. Buettner. 2005. Distinct spatial expression patterns of AP-2alpha and AP-2gamma in non-neoplastic human breast and breast cancer. *Mod. Pathol.* 18:431–438.

Gabriel, B., S. Mildenberger, C.W. Weisser, E. Metzger, G. Gitsch, R. Schule, and J.M. Muller. 2004. Focal adhesion kinase interacts with the transcriptional coactivator FHL2 and both are overexpressed in epithelial ovarian cancer. *Anticancer Res.* 24:921–927.

Grinnell, F. 2000. Fibroblast-collagen-matrix contraction: growth-factor signalling and mechanical loading. *Trends Cell Biol.* 10:362–365.

Gunther, T., C. Poli, J.M. Muller, P. Catala-Lehnen, T. Schinke, N. Yin, S. Vomstein, M. Amling, and R. Schule. 2005. Fhl2 deficiency results in osteopenia due to decreased activity of osteoblasts. *EMBO J.* 24:3049–3056.

Hamm, A., N. Krott, I. Breibach, R. Blindt, and A.K. Bosserhoff. 2002. Efficient transfection method for primary cells. *Tissue Eng.* 8:235–245.

Hinz, B., and G. Gabbiani. 2003. Cell-matrix and cell-cell contacts of myofibroblasts: role in connective tissue remodeling. *Thromb. Haemost.* 90:993–1002.

Ilic, D., Y. Furuta, S. Kanazawa, N. Takeda, K. Sobue, N. Nakatsuji, S. Nomura, J. Fujimoto, M. Okada, and T. Yamamoto. 1995. Reduced cell motility and enhanced focal adhesion contact formation in cells from FAK-deficient mice. *Nature*. 377:539–544.

Jager, R., U. Werling, S. Rimpf, A. Jacob, and H. Schorle. 2003. Transcription factor AP-2gamma stimulates proliferation and apoptosis and impairs differentiation in a transgenic model. *Mol. Cancer Res.* 1:921–929.

Jain, M.K., M.D. Layne, M. Watanabe, M.T. Chin, M.W. Feinberg, N.E. Sibinga, C.M. Hsieh, S.F. Yet, D.L. Stemple, and M.E. Lee. 1998. In vitro system for differentiating pluripotent neural crest cells into smooth muscle cells. *J. Biol. Chem.* 273:5993–5996.

Jayanthi, S., M.T. McCoy, B. Ladenheim, and J.L. Cadet. 2002. Methamphetamine causes coordinate regulation of Src, Cas, Crk, and the Jun N-terminal kinase-Jun pathway. *Mol. Pharmacol.* 61:1124–1131.

Kong, Y., J.M. Shelton, B. Rothermel, X. Li, J.A. Richardson, R. Bassel-Duby, and R.S. Williams. 2001. Cardiac-specific LIM protein FHL2 modifies the hypertrophic response to beta-adrenergic stimulation. *Circulation*. 103:2731–2738.

Lai, C.F., S. Bai, B.A. Uthgenannt, L.R. Halstead, P. McLoughlin, B.W. Schafer, P.H. Chu, J. Chen, C.A. Otey, X. Cao, and S.L. Cheng. 2006. Four and half lim protein 2 (FHL2) stimulates osteoblast differentiation. *J. Bone Miner. Res.* 21:17–28.

Lavrovskii, V.A., and V.A. Razvorotnev. 1976. (A chamber for determination of the rate of macrophage migration under different experimental conditions). *Tsitologiia*. 18:113–116.

Martin, B., R. Schneider, S. Janetzky, Z. Waibler, P. Pandur, M. Kuhl, J. Behrens, K. von der Mark, A. Starzinski-Powitz, and V. Wixler. 2002. The LIM-only protein FHL2 interacts with beta-catenin and promotes differentiation of mouse myoblasts. *J. Cell Biol.* 159:113–122.

Mitra, S.K., D.A. Hanson, and D.D. Schlaepfer. 2005. Focal adhesion kinase: in command and control of cell motility. *Nat. Rev. Mol. Cell Biol.* 6:56–68.

Morlon, A., and P. Sassone-Corsi. 2003. The LIM-only protein FHL2 is a serum-inducible transcriptional coactivator of AP-1. *Proc. Natl. Acad. Sci. USA*. 100:3977–3982.

Muller, J.M., U. Isele, E. Metzger, A. Rempel, M. Moser, A. Pscherer, T. Breyer, C. Holubarsch, R. Buettner, and R. Schule. 2000. FHL2, a novel tissue-specific coactivator of the androgen receptor. *EMBO J.* 19:359–369.

Muller, J.M., E. Metzger, H. Greschik, A.K. Bosserhoff, L. Mercep, R. Buettner, and R. Schule. 2002. The transcriptional coactivator FHL2 transmits Rho signals from the cell membrane into the nucleus. *EMBO J.* 21:736–748.

Park, J., K. Gelse, S. Frank, K. von der Mark, T. Aigner, and H. Schneider. 2006. Transgene-activated mesenchymal cells for articular cartilage repair: a comparison of primary bone marrow-, perichondrium/periosteum- and fat-derived cells. *J. Gene Med.* 8:112–125.

Philippar, U., G. Schratt, C. Dieterich, J.M. Muller, P. Galgoczy, F.B. Engel, M.T. Keating, F. Gertler, R. Schule, M. Vingron, and A. Nordheim. 2004. The SRF target gene Fhl2 antagonizes RhoA/MAL-dependent activation of SRF. *Mol. Cell*. 16:867–880.

Playford, M.P., and M.D. Schaller. 2004. The interplay between Src and integrins in normal and tumor biology. *Oncogene*. 23:7928–7946.

Purcell, N.H., D. Darwis, O.F. Bueno, J.M. Muller, R. Schule, and J.D. Molkentin. 2004. Extracellular signal-regulated kinase 2 interacts with

and is negatively regulated by the LIM-only protein FHL2 in cardiomyocytes. *Mol. Cell. Biol.* 24:1081–1095.

Samson, T., N. Smyth, S. Janetzky, O. Wendler, J.M. Muller, R. Schule, H. von der Mark, K. von der Mark, and V. Wixler. 2004. The LIM-only proteins FHL2 and FHL3 interact with alpha- and beta-subunits of the muscle alpha7beta1 integrin receptor. *J. Biol. Chem.* 279:28641–28652.

Wixler, V., D. Geerts, E. Laplantine, D. Westhoff, N. Smyth, M. Aumailley, A. Sonnenberg, and M. Paulsson. 2000. The LIM-only protein DRAL/FHL2 binds to the cytoplasmic domain of several alpha and beta integrin chains and is recruited to adhesion complexes. *J. Biol. Chem.* 275:33669–33678.

Yanase, M., H. Ikeda, A. Matsui, H. Maekawa, E. Noiri, T. Tomiya, M. Arai, T. Yano, M. Shibata, M. Ikebe, et al. 2000. Lysophosphatidic acid enhances collagen gel contraction by hepatic stellate cells: association with rho-kinase. *Biochem. Biophys. Res. Commun.* 277:72–78.

Yatomi, Y., T. Ohmori, G. Rile, F. Kazama, H. Okamoto, T. Sano, K. Satoh, S. Kume, G. Tigyi, Y. Igarashi, and Y. Ozaki. 2000. Sphingosine 1-phosphate as a major bioactive lysophospholipid that is released from platelets and interacts with endothelial cells. *Blood*. 96:3431–3438.